Proc. Natl. Acad. Sci. USA
Vol. 94, pp. 6965–6970, June 1997
Medical Sciences

Homo- and heterodimeric interactions between the gene products of *PKD1* and *PKD2*

(polycystic kidney disease/yeast two-hybrid system/protein–protein interactions)

LEONIDAS TSIOKAS*†, EMILY KIM†‡, THIERRY ARNOULD*, VIKAS P. SUKHATME*, AND GERD WALZ*§

*Renal Division, Department of Medicine, Beth Israel Deaconess Medical Center, Harvard Medical School, Boston, MA 02215; and ‡Laboratory of Molecular and Developmental Neuroscience, Massachusetts General Hospital, Harvard Medical School, Boston, MA 02114

Communicated by Irving M. London, Massachusetts Institute of Technology, Cambridge, MA, May 1, 1997 (received for review January 3, 1997)

ABSTRACT ***PKD1* and *PKD2* are two recently identified genes that are responsible for the vast majority of autosomal polycystic kidney disease, a common inherited disease that causes progressive renal failure. *PKD1* encodes polycystin, a large glycoprotein that contains several extracellular motifs indicative of a role in cell–cell or cell–matrix interactions, and the *PKD2* encodes a protein with homology to a voltage-activated calcium channel and to PKD1. It is currently unknown how mutations of either protein functionally cause autosomal polycystic kidney disease. We show that PKD1 and PKD2 interact through their C-terminal cytoplasmic tails. This interaction resulted in an up-regulation of PKD1 but not PKD2. Furthermore, the cytoplasmic tail of PKD2 but not PKD1 formed homodimers through a coiled–coil domain distinct from the region required for interaction with PKD1. These interactions suggest that PKD1 and PKD2 may function through a common signaling pathway that is necessary for normal tubulogenesis and that PKD1 may require the presence of PKD2 for stable expression.**

Autosomal dominant polycystic kidney disease (ADPKD) is a common hereditary disease that accounts for 8–10% of end-stage renal disease. ADPKD is genetically heterogeneous with loci mapped to chromosome 16p13.3 (*PKD1*) (1) and to chromosome 4q21–23 (*PKD2*) (2–4), with the likelihood of a third unmapped locus. *PKD1* (5, 6) and *PKD2* (4) have recently been cloned and found to be broadly expressed (4, 7). The predicted PKD1 protein is a glycoprotein with multiple transmembrane domains and a C-terminal cytoplasmic tail of 225 amino acids. The N-terminal extracellular region of ≈2,557 amino acids contains multiple domains that implicate PKD1 in cell–cell or cell–matrix interactions. These include leucine-rich repeats, a C-type lectin domain, 16 immunoglobulin-like repeats, and 4 type III fibronectin-related domains. *PKD2* encodes an integral membrane protein of 968 amino acids containing six transmembrane domains flanked by cytoplasmic N and C termini. Homology of PKD2 to the $\alpha_{1E\text{-}1}$ subunit of a voltage-activated calcium channel (VACC$\alpha_{1E\text{-}1}$) (4) is evident throughout most of the transmembrane domains and the cytoplasmic C-terminal tail, including a potential E-F hand motif. Similarities between PKD1 and PKD2 are restricted to the transmembrane domains I through IV of PKD2. The predicted structures of PKD1 and PKD2, and their similar disease profiles, are highly suggestive of their involvement in a common signaling pathway that links extracellular adhesive events to alterations in ion transport (4).

Although various functional abnormalities have been detected in cultured human epithelial cells isolated from cystic lesions of patients with ADPKD, these observations have not clarified the nature of the aberrant gene products caused by mutations of *PKD1* and *PKD2*. Renal cysts are thought to arise through a process of persistent epithelial proliferation related to the lack of terminal differentiation. Both abnormal growth factor responsiveness (8–12) and the elevated expression of certain oncogenes appear to support this hypothesis (13–16). Recently, loss of heterozygosity was discovered within a subset of cysts for two closely linked polymorphic markers located within the PKD1 gene, indicating that cyst formation in ADPKD1 requires the absence of functional PKD1 protein (17).

On the basis of the overlapping expression patterns of PKD1 and PKD2, the similar disease presentations of the two mutated genes, and predicted protein structures that support a role in signal transduction, we hypothesized that PKD1 and PKD2 are closely associated in a signal transduction pathway. In the present study, we have demonstrated that PKD1 and PKD2 interact through their C-terminal cytoplasmic tails. This interaction resulted in an up-regulation of PKD1 but not PKD2. Furthermore, the cytoplasmic tail of PKD2 but not PKD1 formed homodimers through a region distinct from the domain required for interaction with PKD1. These results are consistent with a mechanism whereby mutations in PKD2 could impede the function of PKD1 and thereby result in a disease presentation similar to that of PKD1 through distinct molecular lesions of a common signaling pathway operational in normal tubulogenesis.

MATERIALS AND METHODS

Constructs and Materials. The C-terminal cytoplasmic domains of wild-type PKD1 and PKD2 were amplified by PCR from KG8 (M. C. Schneider, Brigham and Women's Hospital, Boston, MA) and yj63h09, an expressed sequence tag clone obtained from a human breast library (Genome Systems), respectively. DNA fragments for PKD1 and PKD2 deletion constructs were obtained by PCR-directed introduction of in-frame stop codons at the positions of the amino acids as indicated in Fig. 1. For the yeast two-hybrid analysis, the fragments were cloned by PCR-introduced *Mlu*I–*Not*I sites into pLEX, a derivative of plex202 (18), to generate a LexA fusion protein (bait) or into pCGA, a derivative of pcgatrp2 containing a bacterial transcriptional activator (prey) under the control of the galactose-inducible promoter GAL1 (E.K. and B. Seed, unpublished data). Membrane-bound fusions of

Abbreviations: ADPKD, autosomal dominant polycystic kidney disease; GFP, green fluorescent protein; F, FLAG-tag without leader sequence; sF, FLAG-tag with the leader sequence of preprotrypsin; sIg.7, leader sequence of CD5 followed by the CH_2 and CH_3 domain of human IgG_1 and the transmembrane domain of CD7; CD16.7, extracellular domain of CD16 followed by the transmembrane domain of CD7; BAP2, bacterial alkaline phosphatase; REJ, sea urchin sperm receptor for egg jelly; MBP, maltose-binding protein.

†L.T. and E.K. contributed equally to this work.
§To whom reprint requests should be addressed.

The publication costs of this article were defrayed in part by page charge payment. This article must therefore be hereby marked "*advertisement*" in accordance with 18 U.S.C. §1734 solely to indicate this fact.

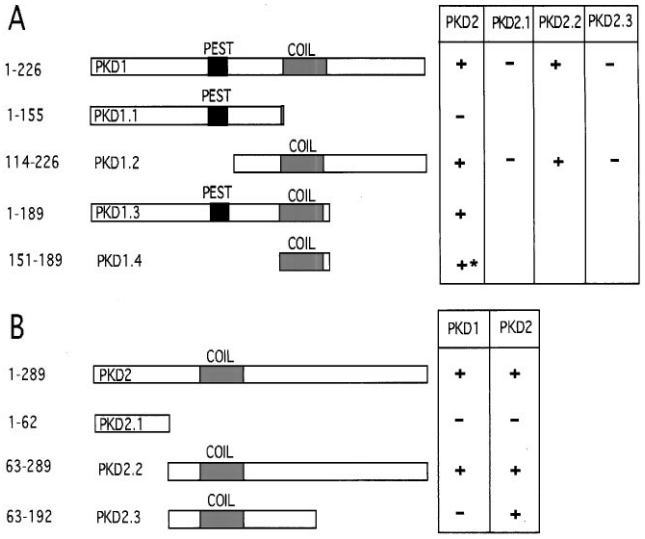

FIG. 1. Mapping the heterodimerization domains of PKD1 and PKD2 (*A*) and the homodimerization domains of PKD2 (*B*) in the yeast two-hybrid system. (*A*) The C-terminal 226 amino acids of PKD1 and progressive C- and N-terminal deletions of this domain were inserted into pLEX. For PKD2 binding assays, the pLex bait constructs and PKD2 prey constructs were sequentially transfected into the yeast strain EGY48 bearing a *lacZ* reporter. Interaction (+) was indicated by β-galactosidase production and leucine prototrophy in yeast; the minimal interacting domain, PKD1.4, caused leucine prototrophy without β-galactosidase production (*). A putative coiled–coil structure is depicted as a shaded box, a potential PEST sequence is depicted as a solid box. (*B*) The C-terminal 289 amino acids of PKD2 and progressive C- and N-terminal deletions of this domain were inserted into pLEX to map the interaction with PKD1 and PKD2. PKD2 binds PKD1 through the C-terminal 97 amino acids. The homodimerization of PKD2 is mediated by a region spanning amino acids 63–192, which contains a putative coiled–coil structure (shaded box).

PKD1 and PKD2 domains were expressed in 293T cells by using a derivative of pCDM8 containing the leader sequence of CD5 fused to the CH_2 and CH_3 domain of human IgG1 followed by the transmembrane region of CD7 (provided by B. Seed, Massachusetts General Hospital, Boston). The C-terminal cytoplasmic domains of PKD1 and PKD2 were fused to the 3′ end of the CD7 transmembrane region. In some experiments, the CD5-CH_2-CH_3 sequences were replaced by the extracellular domain of human CD16 (19–21). The PKD1 construct sF.3TM–PKD1 containing the last three putative transmembrane domains plus the cytoplasmic tail of PKD1 was tagged at its N terminus with the leader sequence of preprotrypsin followed by a FLAG epitope (Kodak). FLAG tags without a leader sequence were used to express cytoplasmic versions of PKD1 and PKD2. A plasmid directing the expression of green fluorescent protein (GFP) (22) was used to monitor transfection efficiency. Sequence identity of the PCR constructs was confirmed by restriction analysis and DNA sequencing. The following antibodies were used for Western blot analysis: the anti-FLAG mouse monoclonal antibody M2 (Kodak), an anti-GFP rabbit polyclonal antiserum (CLONTECH), the anti-α-catenin monoclonal antibody (Transduction Laboratories, Lexington, KY), and the anti-CD16 monoclonal antibody BMA209 (Behring).

Immunofluorescence. To demonstrate surface expression of the constructs CD16.7–PKD1.2 and sIg.7–PKD2, transiently transfected 293T cells were incubated with either phycoerythrin-conjugated anti-CD16 monoclonal antibody (Immunotech, Westbrook, ME) or fluorescein isothiocyanate-conjugated goat anti-human IgG polyclonal antiserum (Cappel) prior to fixation. Cells were washed twice in PBS, fixed in 3% formaldehyde/PBS, and visualized by fluorescence microscopy.

Two-Hybrid Interaction Analysis. Yeast transformation and interaction analysis were performed as described (18). For assessing the interactions of PKD1 and PKD2, pLEX expressing the appropiate fragments of PKD1 and PKD2 were transformed into the yeast strain EGY48/pRB1840 (23) bearing the *lacZ* reporter plasmid JK103 under the control of LexA binding sites. These bait stains were subsequently transformed with pCGA-PKD2 deletion plasmids. Interaction between bait- and prey-encoding fusion proteins was determined by β-galactosidase production and leucine prototrophy of yeast grown in the presence of galactose.

Coimmunoprecipitations. To analyze protein–protein interactions *in vivo*, 293T cells were transiently transfected with 10 μg of plasmid DNA by the calcium phosphate method. After incubation for 24 hr, cells were washed twice with PBS and then lysed in 1 ml of 1% Triton X-100 buffer containing 150 mM NaCl, 10 mM Tris·HCl (pH 7.5), 1 mM EDTA, 1 mM EGTA, 0.2 mM sodium vanadate, 0.2 mM phenylmethylsulfonyl fluoride, 0.5% Nonidet P-40, aprotinin (1 μg/ml), and pepstatin (1 μg/ml). Cell lysates containing equal amounts of total protein were incubated for 1 hr at 4°C with 50 μl of 30% protein A-Sepharose beads (Pharmacia). The beads were washed extensively with lysis buffer and bound proteins were fractionated by SDS/PAGE on 12% gels and transferred to a poly(vinylidene difluoride) membrane (Millipore) with a semi-dry transfer system (Bio-Rad). Western blot analysis was performed with anti-FLAG M2 (10 μg/ml) or anti-CD16 BMA209 (1:5,000 dilution) followed by incubation with horseradish peroxidase-coupled sheep anti-mouse immunoglobulin (Amersham). Immunoglobulin-fusion proteins were directly labeled by horseradish peroxidase-coupled donkey anti-human IgG immunoglobulin (Amersham). Immobilized antibodies were detected by chemiluminescence (Pierce). For analysis of metabolically labeled proteins, 750 μCi (1 Ci = 37 GBq) of [^{35}S]methionine/[^{35}S]cysteine per 1.5 ml of methionine/cysteine-free medium was added to the cells ≈24 hr after transfection. Cells were harvested after 6 hr, and coimmunoprecipitations were performed as above. Labeled proteins were detected by autoradiography after separation on a 12% SDS/PAGE gel. The intensity of the protein bands was recorded by using a Molecular Dynamics PhosphorImager and converted into molar ratios based on the number of methionines and cysteines incorporated into each molecule. For *in vitro* coimmunoprecipitations, [^{35}S]methionine labeled F–PKD2 was generated with the Promega TNT system. A fusion between PKD1.2 and the maltose-binding protein (MBP) was generated, by using a modification of the pmal-c2 vector (New England Biolabs). Ten microliters of the reaction mixture was incubated with 2 μg of MBP–PKD1.2 or with 2 μg of MBP–FIT, an unrelated control protein of equal length (E.K. and B. Seed, unpublished data), immobilized on amylose resin in the presence of 450 μl of reaction buffer [50 mM potassium phosphate, pH 7.5/150 mM KCl/1 mM $MgCl_2$/10% glycerol/1% Triton X-100/*Escherichia coli* lysate (10 mg/ml)/protease inhibitors). The reaction mixture was incubated for 2 hr, washed three times in reaction buffer (0.5% Triton X-100), separated on a SDS/10% polyacrylamide gel, and visualized by autoradiography.

RESULTS

PKD1 Interacts with PKD2 in Yeast. A physical interaction between the C-terminal cytoplasmic domains of PKD1 and PKD2 was observed by using the yeast two-hybrid system (Fig. 1*A*). In this experiment, the C-terminal cytoplasmic domain of PKD1 served as a bait, and the C-terminal cytoplasmic domain of PKD2 was used as a prey. After cotransfection of bait and prey plasmids into yeast cells, interaction was assessed by the

survival of yeast on leucine-deficient medium and the production of β-galactosidase. PKD1 specifically interacted with PKD2 but not with a number of heterologous baits or with itself (data not shown). Further two-hybrid analysis using deletions of PKD1 and PKD2 localized the interacting domain of PKD1 to a 40-amino acids region contained within the last 76 amino acids of PKD1, a region that contains a probable coiled–coil structure (24) (Fig. 1). The domain of PKD2 responsible for binding of PKD1 was found to reside in a region spanning the last 97 amino acids of PKD2 (Fig. 1*A*).

PKD2 Forms Homodimers Through a C-Terminal Cytoplasmic Coiled–Coil Domain in Yeast. The detection of a probable coiled–coil domain in PKD2 outside of the PKD1-binding domain suggested to us a possible mechanism for self-dimerization. The yeast two-hybrid system was used to confirm the homodimerization of PKD2 and to map the domain mediating this interaction (Fig. 1*B*). The formation of PKD2 homodimers was found to be mediated by a domain within amino acids 63–192 of the C terminus. These results indicate that PKD2 interacts with PKD1 through a domain that is distinct from the region of PKD2 required for its homodimerization.

Expression of Recombinant PKD2 Up-Regulates the Expression of PKD1 in Mammalian Cells. Because both PKD1 and PKD2 appear to represent integral membrane proteins that have not yet been expressed in full-length *in vivo* (ref. 25 and L.T., unpublished results), we designed an expression system that targeted the cytoplasmic domains of PKD1 and PKD2 to the plasma membrane by using a single heterologous transmembrane domain. The transmembrane region of human CD7 has been used to anchor cytoplasmic peptides to the plasma membrane while retaining their functional activity (19–21). The C-terminal cytoplasmic tails of PKD1 and PKD2 were each fused to the 3′ end of the CD7 transmembrane domain, which was in turn preceded by the extracellular domains of either CD16 or the leader sequence of CD5 followed by the CH_2 and CH_3 domain of human IgG1 (Fig. 2*A*). Plasmids directing the expression of CD16-CD7 (CD16.7) or CH_2-CH_3-CD7 (sIg.7) fusion proteins were transfected into 293T cells and the surface expression of the individual constructs was demonstrated by immunofluorescence (Fig. 2*B*). In addition, a PKD1 construct bearing three putative C-terminal transmembrane domains and the cytoplasmic tail of PKD1 was tagged at its N terminus with the leader sequence of preprotrypsin followed by the FLAG epitope (sF.3TM–PKD1; Fig. 2*A*). Cytoplasmic versions of both the C-terminal domains of PKD1 and PKD2 were expressed as FLAG-tagged proteins without a proceeding leader sequence (F). These constructs permitted us to analyze the interaction between PKD1 and PKD2 with either or both partners expressed as membrane-bound receptors. We noticed very low levels of expression for F–PKD1 in the lysates of cells cotransfected with the control plasmid sIg.7 (Fig. 3, lane 5). The presence of a potential PEST sequence spanning amino acids 93–109 (26, 27) may mediate this effect since deletion of the first 113 amino acids of the cytoplasmic domain resulted in increased protein levels of F–PKD1.2 (Fig. 3, lanes 3 and 4).

An up-regulation of both membrane-bound and cytoplasmic PKD1 protein levels was detected when plasmids SF.3TM–PKD1, F–PKD1, and F–PKD1.2 were coexpressed with sIg.7–PKD2. This was not apparent for cytoplasmic PKD2; in fact, F–PKD2 protein levels were slightly reduced when cotransfected with sIg.7–PKD2 (see Fig. 5 *A*, lane 2, and *D*, lane 3). To allow a more quantitative assessment of the PKD1 up-regulation in the presence of PKD2, an expression vector encoding GFP was included in the transfection mixture at a constant ratio. Lysates of transfected 293T cells were probed sequentially for FLAG-tagged fusions, GFP, and an endogenous structural protein, α-catenin. The expression of GFP provided a measure for transfection efficiency, and the expression of α-catenin served to normalize for the amount of total protein loaded in each lane. Cotransfection of sIg.7–PKD2 but not sIg.7 resulted in a significant increase of all three PKD1 fusion proteins (Fig. 3, lanes 4, 6, and 8). These results provide indirect evidence that one role of membrane-bound PKD2 may be to interact with and stabilize PKD1.

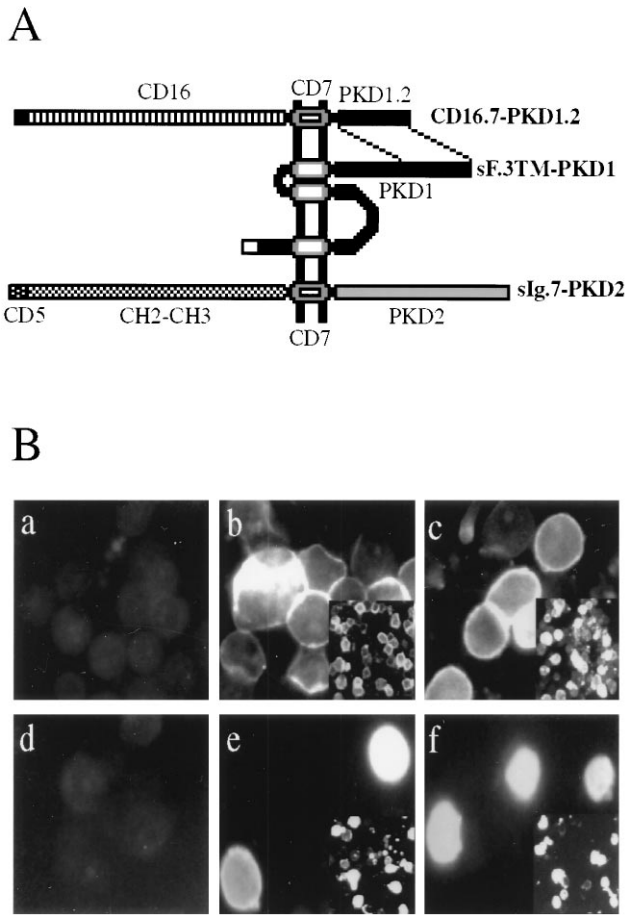

FIG. 2. Construction (*A*) and surface expression (*B*) of membrane-bound PKD1 and PKD2 fusion proteins. (*A*) The C-terminal 113 amino acids of PKD1 (PKD1.2) and the extracellular domain of CD16 were fused to the transmembrane region of CD7 to yield the chimeric integral membrane protein CD16.7–PKD1.2. The construct sF.3TM–PKD1, containing the last three putative transmembrane domains plus the cytoplasmic tail of PKD1, is tagged at its N terminus with the leader sequence of preprotrypsin followed by a FLAG epitope. The membrane-bound fusion of PKD2, sIg.7–PKD2, was generated by fusing the C-terminal 289 amino acids of PKD2 to a cell surface expressed immunoglobulin consisting of the leader sequence of CD5, the CH_2 and CH_3 domain of human IgG1, and the transmembrane region of CD7. (*B*) Surface expression of CD16.7–PKD1.2 and sIg.7–PKD2 fusion proteins. 293T cells were transfected with vector (*a*), CD16.7 (*b*), CD16.7–PKD1.2 (*c*), vector (*d*), sIg.7 (*e*), sIg.7–PKD2 (*f*), and labeled with anti-CD16-fluorescein isothiocyanate (*a–c*) or anti-human IgG-phycoerythrin (*d–f*). Photographs were taken at ×400 magnification under fluorescence microscopy 24 hr after transfection. (*Insets*) Lower magnification (×100) are located in the right lower of *b, c, e,* and *f*. Expression of CD16.7–PKD1.2 (*c*) and sIg.7–PKD2 (*f*) was clearly detected on the surface of unfixed cells.

Heterodimerization Between PKD1 And PKD2. To confirm the results obtained in the yeast two-hybrid assay, 293T cells were cotransfected with combinations of membrane-bound and cytoplasmic versions of PKD1 and PKD2. A specific interaction was detected between F–PKD2 and sIg.7–PKD1.2 (Fig. 4*A*, lane 2), sIg.7–PKD2 and F–PKD1.2 (Fig. 4*A*, lane 4), and sIg.7–PKD2 and F–PKD1 (Fig. 4*A*, lane 6), demonstrating that the PKD2 binding region of PKD1 maps to the most C-terminal 113 amino acids. No interaction was detectable

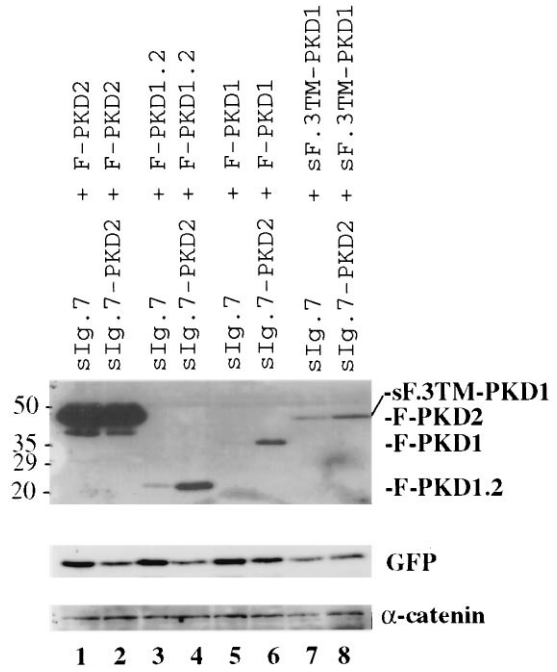

FIG. 3. Up-regulation of PKD1 fusion proteins by membrane-bound PKD2 (sIg.7–PKD2). 293T cells were cotransfected with 4 μg of expression vector for FLAG-tagged PKD1 or PKD2 truncations and 4 μg of expression vector for sIg.7 (control) or sIg.7–PKD2. All transfection mixes contained 2 μg of GFP. Cell lysates were immunoprecipitated with protein A, followed by sequential Western blot analysis with anti-FLAG, anti-GFP, and anti-α-catenin. Increased levels of PKD1 proteins, but not PKD2 protein, were observed (lanes 4, 6, and 8). Control for transfection efficiency was provided by GFP levels that were similar or lower than in control transfections containing sIg.7, and total amount of protein loaded in each lane was monitored by α-catenin expression.

between the FLAG-tagged PKD1 and PKD2 fusion proteins with the control protein sIg.7 (Fig. 4*A*, lanes 1, 3, and 5) or sIg.7–CD40 (data not shown). Thus, membrane-bound PKD1 or PKD2 has the ability to interact with soluble forms of each other. Furthermore, this interaction occurs when both PKD1 and PKD2 are expressed as integral membrane proteins. The fusion protein sF.3TM–PKD1 was used to cotransfect 293T cells in combination with sIg.7–PKD2. Immunoprecipitation with protein A and subsequent Western blot analysis with anti-FLAG antibody showed that sF.3TM–PKD1 was coprecipitated with sIg.7–PKD2 (Fig. 4*B*, lane 1) and not with the control protein sIg.7–CD40 (Fig. 4*B*, lane 2). To rule out a nonspecific interaction between the CH_2-CH_3 domains of sIg.7–PKD2 and the FLAG epitope, we cotransfected sIg.7–PKD2 and a FLAG-tagged version of bacterial alkaline phosphatase (BAP2) and showed that sIg.7–PKD2 and F–BAP2 did not coimmunoprecipitate (Fig. 4*B*, lane 3). Having demonstrated that sF.3TM–PKD1, the three-membrane spanning version of PKD1, specifically associates with membrane-anchored PKD2, we confirmed the association of the cytoplasmic tails of PKD1 and PKD2 by coexpressing two different membrane-bound forms of PKD1.2, CD16.7–PKD1.2 and sIg.7–PKD2, in 293T cells. Cell lysates were immunoprecipitated with protein A and coprecipitating sIg.7–PKD2 was detected by immunoblotting with anti-CD16 (Fig. 4*B*, lane 6). No association was seen between sIg.7–PKD2 and CD16.7 (Fig. 4*B*, lane 4) or sIg.7–CD40 and CD16.7–PKD1.2 (Fig. 4*B*, lane 5). These results indicate that the C-terminal tails of PKD1 and PKD2 associate in mammalian cells. To determine whether other cellular proteins participate in the interaction between PKD1 and PKD2, coimmunoprecipitation experiments were performed with ^{35}S-labeled 293T cells. Immunoprecipitation of F–PKD1.2 with anti-FLAG M2 resulted in the coimmunoprecipitation of sIg.7–PKD2 (Fig. 5*A*, lane 1), confirming the results obtained by Western blot analysis. In addition, a faint ≈50-kDa protein appeared in the precipitates containing F–PKD1.2 and sIg.7–PKD2 (Fig. 5*A*, lane 1),

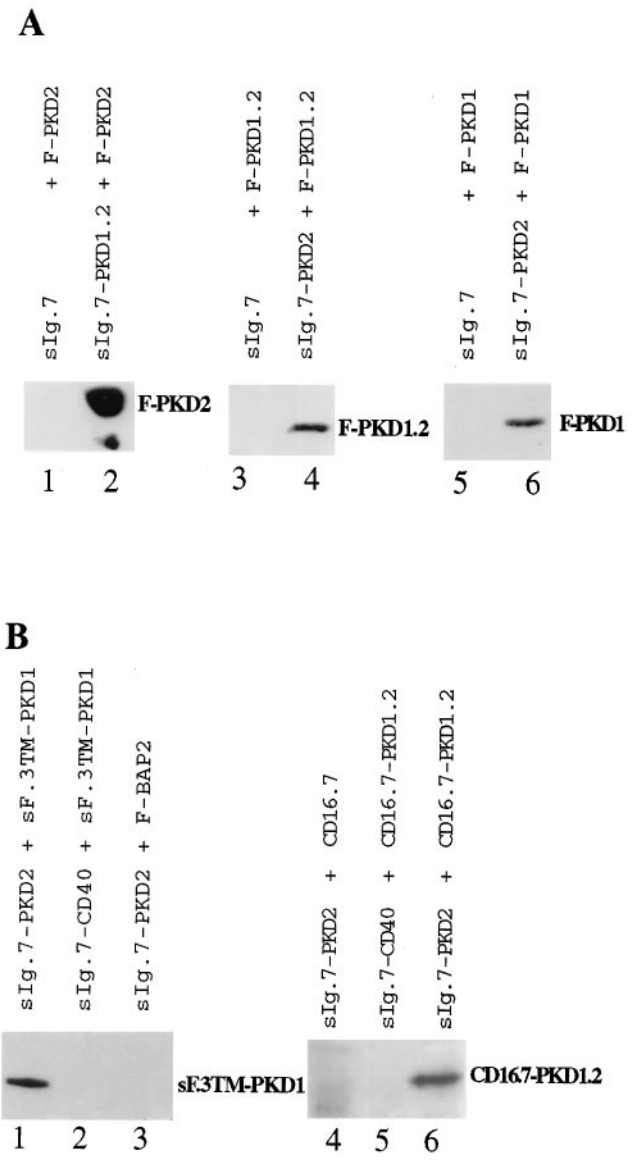

FIG. 4. Heterodimerization of PKD1 and PKD2 *in vivo*. (*A*) Coimmunoprecipitation of membrane-bound chimeric PKD1 and PKD2 proteins with cytoplasmic PKD2 and PKD1 fusion proteins, respectively. 293T cells were transfected with the indicated combinations of expression vectors for PKD1 and PKD2, and cell lysates were immunoprecipitated with protein A, followed by Western blot analysis with anti-FLAG. sIg.7–PKD1.2 interacted with F–PKD2 (lane 2) but not with the sIg.7 control protein (lane 1). The interaction between sIg.7–PKD2 and F–PKD1.2 is demonstrated in lane 4; the interaction between sIg.7–PKD2 and F–PKD1 is shown in lane 6. Neither F–PKD1.2 nor F–PKD1 interacted with the sIg.7 control protein. (*B*) Coimmunoprecipitation of membrane-bound fusion proteins of PKD2 and PKD1. 293T cells were transfected with the expression vectors indicated above. Immunoprecipitations were performed with protein A, followed by Western blot analysis with anti-FLAG (lanes 1–3) or anti-CD16 (lanes 4–6). Lane 1 demonstrates the interaction with sIg.7–PKD2 and sF.3TM–PKD1. No interaction was detectable between sF.3TM–PKD1 and sIg.7–CD40 or between sIg.7–PKD2 and F–BAP2. Lane 6 shows the interaction between the two membrane-bound fusion proteins CD16.7–PKD1.2 and sIg.7–PKD2. No interaction was detectable with the control proteins CD16.7 (lane 4), or sIg.7–CD40 (lane 5).

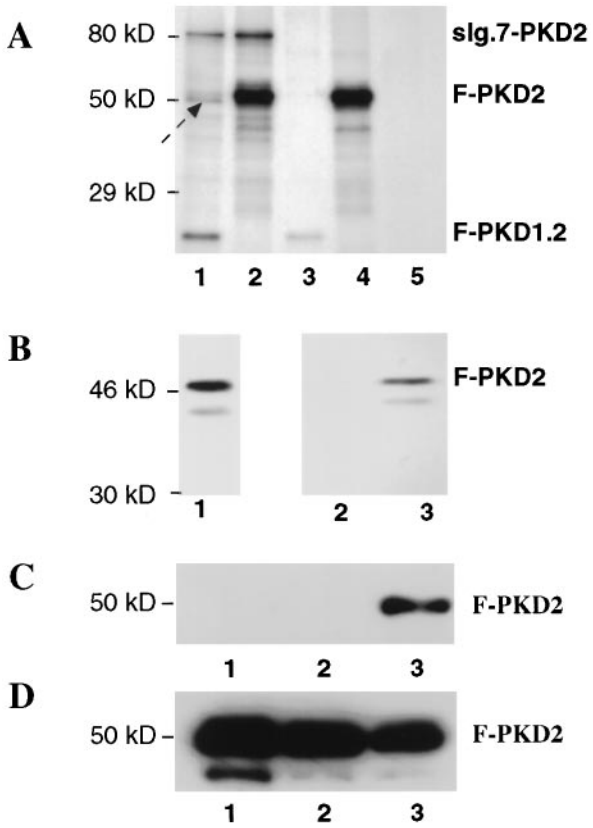

FIG. 5. Hetero- and homodimerization of PKD1 and PKD2. (*A*) Coimmunoprecipitations of ^{35}S-labeled PKD1 and PKD2 fusions proteins. 293T cells were transfected with sIg.7–PKD2 and F–PKD1.2 (lane 1), sIg.7–PKD2 and F–PKD2 (lane 2), sIg.7 and F–PKD1.2 (lane 3), sIg.7 and F–PKD2 (lane 4), or remained untransfected (lane 5). Cells were harvested after a 6-hr chase with [^{35}S]methionine/cysteine. Immunoprecipitations were performed with anti-FLAG M2 affinity gel. The arrow marks a putative 50-kDa protein present in lane 1 (and potentially in lanes 2 and 4), which appears to associate with PKD2 or the PKD1–PKD2 complex. Similar results were obtained with reciprocal immunoprecipitation using protein A to immunoprecipiate the IgG-tagged constructs (data not shown). (*B*) Coimmunoprecipitation of ^{35}S-labeled F–PKD2 with MBP–PKD1.2 fusion protein. F–PKD2 was *in vitro* transcribed and translated (lane 1). An aliquot of the reaction mixture was then incubated with a control MBP–protein (lane 2) or MBP–PKD1.2 (lane 3). (*C*) Homodimerization of PKD2 *in vivo*. 293T cells were cotransfected with sIg.7 and F–PKD2 (lane 1), sIg.7–CD40 and F–PKD2 (lane 2), and sIg.7–PKD2 and F–PKD2 (lane 3). Lysates were immunoprecipitated with protein A, and bound proteins were blotted with anti-FLAG. (*D*) Cell lysates demonstrating comparable expression of the F–PKD2 fusion protein in all three conditions (lanes 1–3 as in *C*).

potentially in precipitates of F–PKD2 and sIg.7–PKD2 (Fig. 5*A*, lane 2), and in F–PKD2 alone (Fig. 5*A*, lane 4), indicating that other cellular protein(s) may coimmunoprecipitate with PKD2 or the PKD1–PKD2 complex. To exclude the possibility that a third cellular protein is required for the interaction between PKD1 and PKD2, we performed coimmunoprecipitations *in vitro* with a recombinant MBP–PKD1.2 fusion protein. Fig. 5*B* demonstrates that *in vitro* transcribed and translated [^{35}S]methionine-labeled F–PKD2 bound to PKD1.2 (Fig. 5*B*, lane 3), but not to an unrelated control protein of similar length (Fig. 5*B*, lane 2). Collectively, these results indicate that the interaction between PKD1 and PKD2 does not require additional cellular proteins.

Homodimerization of PKD2 *in Vivo*. Whereas no homodimerization between PKD1 was detectable in either the yeast two-hybrid system or by coimmunoprecipitation in 293T cells, PKD2 was found to homodimerize in both systems. 293T cells were cotransfected with sIg.7–PKD1.2 or sIg.7 and F–PKD1.2, lysates were immunoprecipitated with protein A, and bound proteins were immunoblotted with anti-FLAG. No interaction was detectable between the cytoplasmic and membrane-anchored versions of PKD1 (data not shown). However, in a similar experiment, cotransfection of sIg.7–PKD2 and F–PKD2 in 293T cells resulted in coimmunoprecipitation of F–PKD2 (Fig. 5*C*, lane 3). This interaction was specific and did not occur when F–PKD2 was coexpressed with sIg.7 or sIg.7–CD40 (Fig. 5*C*, lanes 1 and 2). Thus, the C terminus of PKD2 forms homodimers and heterodimers with the C terminus of PKD1. This is in agreement with results from the two-hybrid analysis, which showed that PKD1 and PKD2 bind to nonoverlapping sites within the C terminus of PKD2.

DISCUSSION

Two genes responsible for ADPKD have recently been identified (4, 5) and sequence analysis of *PKD1* and *PKD2* has fueled speculation over the mechanism by which mutations of these two genes cause a similar presentation of polycystic kidney disease associated with liver cysts and cerebral aneurysm. Several structural elements found in the extracellular domain of PKD1 point to a role in cell–cell and/or cell–matrix interaction: a leucine-rich region, the C-type lectin domain, the repetitive Ig-like domains, and putative fibronectin type III repeats found in other cell adhesion molecules (6). In addition, the extracellular region of PKD1 contains a region (amino acids 2,146–2,882) with significant homology to the sea urchin sperm receptor for egg jelly (REJ) (28), an integral membrane protein whose function is coupled to calcium channels: binding of monoclonal antibodies to REJ initiates the acrosome reaction in sperm by increasing the level of intracellular calcium, a prerequisite for subsequent Na^+/H^+ exchange (28). Interestingly, the combination of Ig-like domains and fibronectin type III repeats is present in the neural cell adhesion molecule and L1, a class of cellular adhesion molecules that translate extracellular events into the activation of L- and N-type neuronal calcium channels (29). Homology between PKD2 and the $\alpha_{1E\text{-}1}$ subunit of voltage-activated calcium channels throughout most of the transmembrane pore-forming domains is equally suggestive of a signal transduction cascade involving PKD1 and PKD2. On the basis of the structural elements and the overlapping clinical presentation of ADPKD1 and ADPKD2, we conjecture that PKD1 and PKD2 operate in a common signaling pathway, transducing extracellular adhesive events into alterations in ion transport.

To begin to elucidate the molecular mechanisms underlying ADPKD, we evaluated the interaction of PKD1 and PKD2 by using the yeast two-hybrid system and *in vivo* and *in vitro* coimmunoprecipitation assays. The association of the two proteins in all three systems supports a model in which the two gene products participate in a common signaling pathway. We used deletional analysis to define sequences within the cytoplasmic domains that are required for binding. A probable coiled–coil structure in PKD1 was found to be essential and sufficient for interaction with PKD2, and a probable coiled–coil structure in PKD2 was located in the domain required for its homodimerization. Since PKD2 has six membrane spans, the self-associating domain could help mediate the homomultimeric complexing necessary for function as an ion channel in a configuration similar to that of potassium channels (30).

One intriguing motif is a potential PEST sequence in the C terminus of PKD1 that appears to target PKD1 for rapid degradation. Deletion of this sequence, as in the construct CD16.7–PKD1.2, resulted in increased protein levels and stable cell surface expression. Several PKD1 versions were found to be up-regulated in the presence of PKD2. A similar up-regulation of α- and β-catenin has been documented in which catenin–cadherin complex formation prevents β-cate-

nin degradation (31, 32). It is possible that during tubulogenesis, stable expression of PKD1 depends upon the presence of PKD2. In this scenario, mutations of PKD1 and PKD2 that compromise protein–protein interaction would interupt the signal transduction cascade and enhance PKD1 degradation. In support of this model is a reported ADPKD mutation that deletes the C-terminal 76 amino acids of PKD1 (33), a domain we found essential for interaction with PKD2. These results suggest that protein stability resulting from the formation of a multimeric complex consisting of PKD1–PKD2 heteromers and PKD2–PKD2 homomultimers may be essential for normal tubulogenesis.

Collectively, these data support the hypothesis that PKD1 and PKD2 participate in a common signaling pathway that prevents cyst formation (4, 17). If PKD2 indeed functions as a voltage-gated ion channel, it is possible that extracellular events sensed by PKD1 could regulate PKD2 channel activity through interactions between the C-terminal cytoplasmic domains of PKD1 and PKD2, and a more N-terminal coiled–coil structure in PKD2 may mediate homomultimeric complexing PKD2 required for the formation of a functional channel.

Note Added in Proof. Qian *et al.* demonstrated the interaction between PKD1 and PKD2 in yeast and *in vitro* (34).

We thank Michael C. Schneider for the KG8 clone and Brian Seed for several constructs and expression cassettes. We thank Steven A. Bossone, Herbert Cohen, Bertrand Knebelmann, and other members of the lab for helpful comments. E.K. was supported by Public Health Service Grant MH-01147, and T.A. was supported by a Research Fellowship of the Belgian American Educational Foundation. This work was supported by National Institutes of Health Grant RO1-DK-51060 (V.P.S.) and a grant from the Polycystic Kidney Research Foundation (G.W.).

1. Reeders, S. T., Breuning, M. H., Davies, K. E., Nicholls, R. D., Jarman, A. P., Higgs, D. R., Pearson, P. L. & Weatherall, D. J. (1985) *Nature (London)* **317,** 542–544.
2. Kimberling, W. J., Kumar, S., Gabow, P. A., Kenyon, J. B., Connolly, C. J. & Somlo, S. (1993) *Genomics* **18,** 467–472.
3. Peters, D. J., Spruit, L., Saris, J. J., Ravine, D., Sandkuijl, L. A., Fossdal, R., Boersma, J., van Eijk, R., Norby, S., Constantinou-Deltas, C. D., Pierides, A., Brissenden, J. E., Frants, R. R., van Ommen, G.-J. B. & Breuning, M. H. (1993) *Nat. Genet.* **5,** 359–362.
4. Mochizuki, T., Wu, G., Hayashi, T., Xenophontos, S. L., Veldhuisen, B., Saris, J. J., Reynolds, D. M., Cai, Y., Gavow, P. A., Pierides, A., Kimberling, W. J., Breuning, M. H., Deltas, C. C., Peters, D. J. M. & Somlo, S. (1996) *Science* **272,** 1339–1342.
5. The International Polycystic Kidney Disease Consortium (1995) *Cell* **81,** 289–298.
6. Hughes, J., Ward, C. J., Peral, B., Aspinwall, R., Clark, K., San Millan, J. L., Gamble, V. & Harris, P. C. (1995) *Nat. Genet.* **10,** 151–160.
7. Ward, C. J., Turley, H., Ong, A. C. M., Comley, M., Biddolph, S., Chetty, R., Ratcliffe, P. J., Gatter, K. & Harris, P. C. (1996) *Proc. Natl. Acad. Sci. USA* **93,** 1524–1528.
8. Wilson, P. D. (1991) *Am. J. Kidney Dis.* **17,** 634–637.
9. Wilson, P. D., Sherwood, A. C., Palla, K., Du, J., Watson, R. & Norman, J. T. (1991) *Am. J. Physiol.* **260,** F420–F430.
10. Wilson, P. D. & Burrow, C. R. (1992) *Adv. Nephrol. Necker. Hosp.* **21,** 125–142.
11. Wilson, P., Falkenstein, D., Gatti, L., Eng, E. & Burrow, C. (1995) *Kidney Int.* **47,** 724–725.
12. Du, J. & Wilson, P. D. (1995) *Am. J. Physiol.* **269,** C487–C495.
13. Cowley, B. D., Jr., Chadwick, L. J., Grantham, J. J. & Calvet, J. P. (1991) *J. Am. Soc. Nephrol.* **1,** 1048–1053.
14. Rankin, C. A., Grantham, J. J. & Calvet, J. P. (1992) *J. Cell. Physiol.* **152,** 578–586.
15. Schaffner, D. L., Barrios, R., Massey, C., Banez, E. I., Ou, C. N., Rajagopalan, S., Aguilar-Cordova, E., Lebovitz, R. M., Overbeek, P. A. & Lieberman, M. W. (1993) *Am. J. Pathol.* **142,** 1051–1060.
16. Trudel, M., D'Agati, V. & Constantini, F. (1991) *Kidney Int.* **39,** 665–671.
17. Qian, F., Watnick, T. J., Onuchic, L. F. & Germino, G. G. (1996) *Cell* **87,** 979–987.
18. Stanger, B., Leder, P., Lee, T., Kim, E. & Seed, B. (1995) *Cell* **81,** 513–523.
19. Kolanus, W., Romeo, C. & Seed, B. (1993) *Cell* **74,** 171–183.
20. Romeo, C., Kolanus, W., Amiot, M. & Seed, B. (1992) *Cold Spring Harbor Symp. Quant. Biol.* **57,** 117–125.
21. Romeo, C., Amiot, M. & Seed, B. (1992) *Cell* **68,** 889–897.
22. Haas, J., Park, E. C. & Seed, B. (1996) *Curr. Biol.* **6,** 315–324.
23. Gyuris, J., Golemis, E., Chertkov, H. & Brent, R. (1993) *Cell* **75,** 791–803.
24. Lupas, A., van Dyke, M. & Stock, J. (1991) *Science* **252,** 1162–1164.
25. Ibraghimov-Beskrovnaya, O., Dackowski, W., Petry, L., Burn, T., Connors, T., van Raay, T., Qian, F., Onuchic, L., Watnik, T., Piontek, K., Hakim, R., Landes, G., Germino, G. & Klinger, K. (1996) *J. Am. Soc. Nephrol.* **7,** 1599 (abstr.).
26. Rechsteiner, M. (1988) *Adv. Enzyme Regul.* **27,** 135–51.
27. Rechsteiner, M. (1990) *Semin. Cell Biol.* **1,** 433–440.
28. Moy, G. W., Mendoza, L. M., Schulz, J. R., Swanson, W. J., Glabe, C. G. & Vacquier, V. D. (1996) *J. Cell Biol.* **133,** 809–817.
29. Doherty, P., Ashton, S. V., Moore, S. E. & Walsh, F. S. (1991) *Cell* **67,** 21–33.
30. Xu, J., Yu, W., Jan, Y. N., Jan, L. Y. & Li, M. (1995) *J. Biol. Chem.* **270,** 24761–24768.
31. Hinck, L., Nathke, I. S., Papkoff, J. & Nelson, W. J. (1994) *J. Cell Biol.* **125,** 1327–1340.
32. Nakagawa, S. & Takeichi, M. (1995) *Development (Cambridge, U.K.)* **121,** 1321–1332.
33. Peral, B., San Millan, J. L., Ong, A. C., Gamble, V., Ward, C. J., Strong, C. & Harris, P. C. (1996) *Am. J. Hum. Genet.* **58,** 86–96.
34. Qian, F., Germino, F. J., Cai, Y., Zhang, X., Somlo, S. & Germino, G. G. (1997) *Nat. Genet.*, in press.